Simultaneous and Rapid Microwave Synthesis of Polyacrylamide−Metal Sulfide (Ag2S, Cu2S, HgS) Nanocomposites

ARTICLE *in* THE JOURNAL OF PHYSICAL CHEMISTRY C · FEBRUARY 2007

Impact Factor: 4.77 · DOI: 10.1021/jp0677851

5 AUTHORS, INCLUDING:

Ying-Jie Zhu
Chinese Academy of Sciences
216 PUBLICATIONS **6,985** CITATIONS
SEE PROFILE

Ming-Guo Ma
Beijing Forestry University
86 PUBLICATIONS **1,399** CITATIONS
SEE PROFILE

Simultaneous and Rapid Microwave Synthesis of Polyacrylamide−Metal Sulfide (Ag_2S, Cu_2S, HgS) Nanocomposites

Jie-Fang Zhu, Ying-Jie Zhu,* Ming-Guo Ma, Li-Xia Yang, and Lian Gao

State Key Laboratory of High Performance Ceramics and Superfine Microstructure, Shanghai Institute of Ceramics, Chinese Academy of Sciences, Shanghai 200050, People's Republic of China

Received: November 22, 2006; In Final Form: January 5, 2007

Polyacrylamide−metal sulfide (Ag_2S, Cu_2S, HgS) nanocomposites with metal sulfide nanoparticles homogeneously dispersed in the polyacrylamide (PAM) matrix have been successfully synthesized using corresponding metal salt, sulfur powder, and acrylamide monomer (AM) in ethylene glycol (EG) by microwave heating. This method is based on the simultaneous formation of metal sulfide nanoparticles and polymerization of the AM, leading to a homogeneous distribution of metal sulfide nanoparticles in PAM matrix without aggregation. EG acts simultaneously as a solvent, a microwave absorber, and a reductant; thus no additional reductant is needed. Another advantage is that no initiator for AM polymerization and no surfactant for the stabilization of these metal sulfide nanoparticles are necessary. The products are characterized by X-ray powder diffraction (XRD), transmission electron microscopy (TEM), Fourier transform infrared (FT-IR), ultraviolet visible (UV−vis) absorption spectra, photoluminescence (PL), thermogravimetric (TG), and differential scanning calorimetric analysis (DSC). The present method may be extended to prepare other polymer−metal sulfide nanocomposites.

Introduction

Recently, polymer−metal sulfide nanocomposites have received much attention due to their interesting optical, electrical, and mechanical properties.[1−14] In these nanocomposites, nanoparticles with high specific surface area and unsaturated atoms may interact with the polymer, leading to the enhancement of properties of the nanocomposite. These nanocomposites are considered to be interesting functional materials with many potential applications in various fields.

To realize the practical applications of the nanocomposites, it is desirable to develop novel, simple, fast, and low-cost methods for the synthesis of these nanocomposites. The control over nanoparticle size, size distribution, and dispersity is very important for the synthesis of high performance nanocomposites. Conventionally, polymerization of the organic monomer and formation of metal sulfide particles were conducted separately, and then the polymer and metal sulfide particles were mixed together, leading to the inhomogeneous mixing of the polymer and metal sulfide particles and severe aggregation of metal sulfide particles and uneven properties in the composites. In some cases, relatively high temperatures or pressures were needed, which made the preparation complex, difficult, and high-cost. Nanocomposites were also synthesized by preparation of metal sulfide nanoparticles in situ in the presence of the pre-prepared polymer. Finally, the nanocomposites were obtained from the dispersion of nanoparticles in polymer solution by coprecipitation or solvent evaporation.[3,4] There have been a few reports on the simultaneous formation of metal sulfide nanoparticles and polymerization of the monomer. For example, PAM−CdS and PAM−PbS were synthesized by a simultaneous formation of CdS or PbS and polymerization of AM in the presence of the initiator of 2,2′-azobisisobutyronitrile.[5,6] Ultraviolet irradiation, γ-irradiation, and microwave were applied to synthesize polymer−metal sulfide nanocomposites.[7−15] PAM−MS (M = Cd, Zn, Pb) nanocomposites were prepared by in situ ultraviolet irradiation in the presence of the initiator of 2,2′-azobisisobutyronitrile for 24 h.[14] γ-Irradiation was used to prepare PAM−CdS nanocomposite.[10] Microwave was used to prepare polymer−metal sulfide nanocomposites, in which poly(*N*-vinylcarbazole)−CdS nanocomposites were prepared via an in situ microwave irradiation method. Thiourea, 2,2′-azobisisobutyronitrile, and pyridine were used as the S resource, initiator, and solvent, respectively.[15] Simultaneous formation of metal sulfide nanoparticles and polymerization of the monomer led to homogeneous dispersion of metal sulfide nanoparticles with a narrow size distribution in the polymer matrix. Unfortunately, commercial applications of simultaneous preparation methods mentioned above are limited due to the requirement of the γ-ray source, relatively long preparation time, or the use of initiators.

The application of microwave heating in the synthesis of nanostructures is a fast growing research area.[16−18] Since the first report of microwave-assisted synthesis in 1986, the microwave heating has been accepted as a promising method for rapid volumetric heating, higher reaction rate and selectivity, short reaction time, and high yield as compared to conventional heating methods. This has opened up the possibility of realizing fast preparation of materials in a very short time. Despite these advantages, microwave simultaneous synthesis of polymer−metal sulfide nanocomposites has little been reported, except poly(*N*-vinylcarbazole)−CdS nanocomposites[15] mentioned above.

In this study, we report in detail the fast microwave-assisted synthesis of PAM−metal sulfide (Ag_2S, Cu_2S, HgS) nanocomposites using corresponding metal salt, sulfur powder, and acrylamide (AM) in the solvent of ethylene glycol (EG). This method is based on the one-step simultaneous formation of metal sulfide nanoparticles and polymerization of the AM, leading to

* Corresponding author. Tel.: +86-21-52412616. Fax: +86-21-52413122. E-mail: y.j.zhu@mail.sic.ac.cn.

10.1021/jp0677851 CCC: $37.00
Published on Web 02/20/2007

a homogeneous distribution of metal sulfide nanoparticles in PAM matrix. EG acts as a solvent, a microwave absorbent, and a reducing reagent; thus no additional reductant is needed. Another advantage is that no initiator for AM polymerization and no surfactant for stabilization of metal sulfide nanoparticles are needed. This makes it possible to avoid subsequent complicated workup procedures for removal of these additives, leading to rapidness, simplicity, and low-cost in the preparation of polymer−metal sulfide nanocomposites.

Experimental Section

Chemicals used in the experiments were analytical reagents and were purchased and used without further purification. In a typical procedure, a certain amount of metal salt ($AgNO_3$, $Cu(NO_3)_2 \cdot 3H_2O$, or $Hg(NO_3)_2 \cdot H_2O$), excessive sulfur powder, and 10.662 g of AM were dispersed in 50 mL of EG under magnetic stirring. The suspension was rapidly microwave-heated to a given temperature (125 or 190 °C), kept at this temperature for a given time, and then cooled down to room temperature naturally. The details of the amount of metal salt, the reaction temperature, and time for each sample are given in the following text. It should be mentioned that the sulfur powder is melted above 115 °C. After the removal of residual sulfur powder by funnel filtration, the stable colloidal solution was obtained. Next, 50 mL of ethanol was added to 10 mL of the colloidal solution to form a precipitate. The product was filtered, washed with ethanol three times, dried in air at 70 °C, and ground into a powder by a mortar. The microwave oven (2.45 GHz, maximum power 300 W) used was a focused single-mode microwave synthesis system (Discover, CEM, USA), which was equipped with a magnetic stirrer and a water-cooled condenser. Temperature was controlled by automatically adjusting the microwave power.

X-ray powder diffraction (XRD) patterns were recorded using a D/max 2550 V X-ray diffractometer with Cu Kα radiation ($\lambda = 1.54178$ Å) and a graphite monochromator, operating at 40 kV and 200 mA. Samples were supported on a single-crystalline silicon holder. Transmission electron microscopy (TEM) and high-resolution transmission electron microscopy (HRTEM) micrographs were taken with a JEOL JEM-2100F field emission transmission electron microscope using an accelerating voltage of 200 kV. For TEM observation, the sample powder was dispersed in ethanol by ultrasonic irradiation, and a drop of the suspension was placed onto a carbon-coated copper grid. The deposit was dried in air prior to TEM observation. The energy-dispersive X-ray spectroscopy (EDS) attached to a transmission electron microscope was used to analyze the composition of samples. The composition of PAM−Cu_2S nanocomposite was determined on Al holder with an accelerating voltage of 20 kV by EDS (Oxford INCA) attached to an EPMA-8705 Electron Probe Microanalyzer (Shimadzu). Fourier transform infrared (FTIR) spectra were collected on a Nicolet-Nexus spectrometer, and the KBr disk method was employed. Ultraviolet visible (UV−vis) absorption spectra were obtained with a Techcomp UV2300 spectrophotometer. The solution of the sample was diluted by EG, and then put in a quartz cuvette with 1 cm optical path length for the measurement. Photoluminescence (PL) spectra of the diluted colloids of the nanocomposites were taken on a Perkin-Elmer LS 55 luminescence spectrometer at room temperature. The samples were placed in a quartz cuvette with 1 cm optical path length for the measurement. Differential scanning calorimetric analysis (DSC) and thermogravimetric analysis (TG) were carried out with a STA-409PC/4/H Luxx simultaneous TG-DTA/DSC apparatus (Netzsch, Germany) at a heating rate of 5 °C min^{-1} under 40 mL min^{-1} of flowing high-purity N_2.

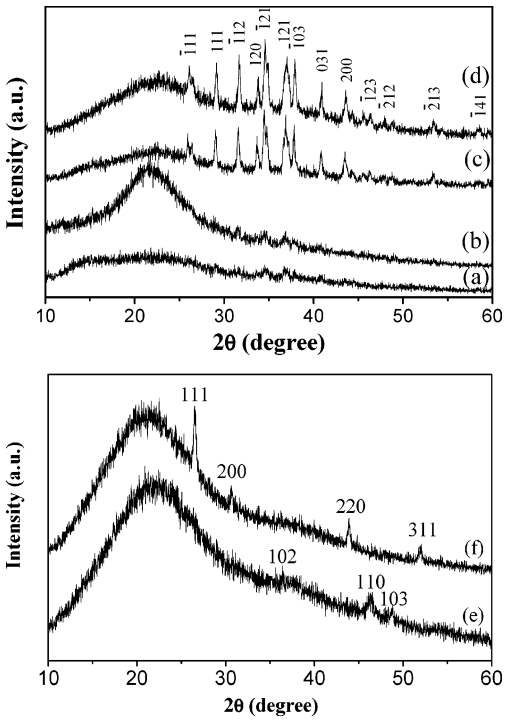

Figure 1. (a)−(d) XRD patterns of PAM−Ag_2S nanocomposite prepared by microwave heating an EG (50 mL) solution containing: (a) 2 mmol of $AgNO_3$, 2 mmol of S, and 0.15 mol of AM at 125 °C for 15 min; (b) 2 mmol of $AgNO_3$, 2 mmol of S, and 0.15 mol of AM at 125 °C for 60 min; (c) 2 mmol of $AgNO_3$, 2 mmol of S, and 0.15 mol of AM at 190 °C for 15 min; (d) 10 mmol of $AgNO_3$, 10 mmol of S, and 0.15 mol of AM at 125 °C for 15 min; (e) XRD pattern of PAM−Cu_2S nanocomposite prepared by microwave heating an EG (50 mL) solution containing 2 mmol of $Cu(NO_3)_2 \cdot 3H_2O$, 2 mmol of S, and 0.15 mol of AM at 190 °C for 15 min; and (f) XRD pattern of PAM−HgS nanocomposite prepared by microwave heating an EG (50 mL) solution containing 1 mmol of $Hg(NO_3)_2 \cdot H_2O$, 2 mmol of S, and 0.15 mol of AM at 190 °C for 15 min.

Results and Discussion

Figure 1a−d shows the XRD patterns of PAM−Ag_2S nanocomposites synthesized under different conditions. A broad peak centers at about 23°, which is assigned to the PAM polymer phase.[19] All other peaks in XRD patterns can be indexed to a monoclinic Ag_2S (JCPDS No. 14-0072), indicating the formation of PAM−Ag_2S nanocomposite. No peaks indexed to elemental Ag or S are found in all XRD patterns, even in the case of the most amount of reactants in Figure 1d, indicating the complete reaction of reduced Ag and removal of residual S. The broadening of the peaks at about 34.4° and 36.8°, which correspond to the diffraction of ($\bar{1}21$) and (121) crystal faces of monoclinic Ag_2S, indicates that Ag_2S particles in the PAM matrix are very small. In Figure 1a, the peaks indexed to Ag_2S are visible but very weak, which can be ascribed to the covering of PAM. The signals of Ag_2S become obvious and clear with increasing amount of Ag_2S (Figure 1d). The size and crystallinity of Ag_2S increased with the reaction temperature, as clearly illustrated by the more intense and narrower peaks in Figure 1c. PAM−Cu_2S (Figure 1e, JCPDS No. 46-1195, hexagonal Cu_2S) and PAM−HgS (Figure 1f, JCPDS No. 06-0261, face-centered cubic (fcc) HgS) nanocomposites can also be synthesized by this method. These results suggest that the method

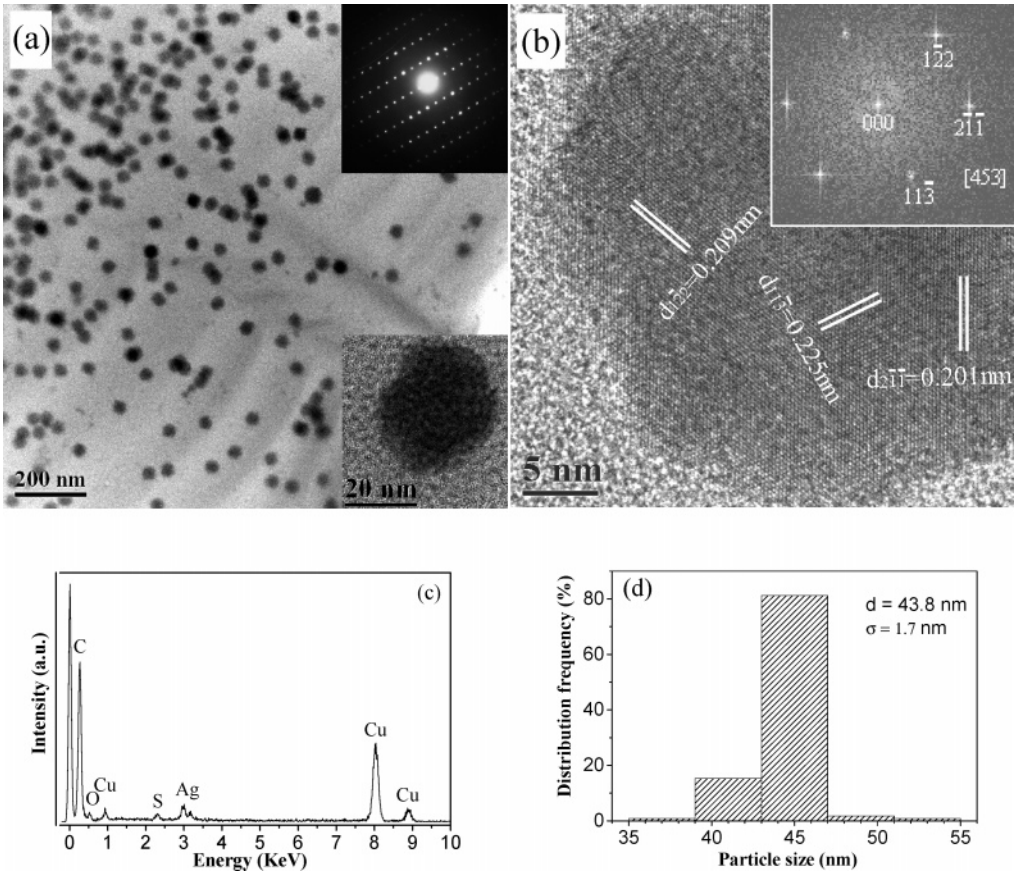

Figure 2. (a) TEM micrograph of PAM−Ag_2S nanocomposite prepared by microwave heating an EG (50 mL) solution containing 2 mmol of $AgNO_3$, 2 mmol of S, and 0.15 mol of AM at 125 °C for 15 min, the selected area electron diffraction (SAED) pattern of an individual Ag_2S nanoparticle (upper inset), and the magnified TEM micrograph of an individual nanoparticle (lower inset); (b) HRTEM image of the edge of an individual Ag_2S nanoparticle (inset: fast Fourier transform (FFT) pattern of the image); (c) EDS spectrum of PAM−Ag_2S nanocomposite; and (d) the histogram of Ag_2S particle size distribution in the nanocomposite.

reported here is effective to synthesize PAM−metal sulfide nanocomposites.

Figure 2a shows the TEM micrograph of the PAM−Ag_2S nanocomposite prepared by microwave heating an EG (50 mL) solution containing 2 mmol of $AgNO_3$, 2 mmol of S, and 0.15 mol of AM at 125 °C for 15 min. One can see that spherical Ag_2S nanoparticles were homogeneously dispersed in the PAM matrix. The simultaneous formation of Ag_2S nanoparticles and polymerization of the AM monomer leads to a homogeneous distribution of Ag_2S nanoparticles in the PAM matrix. The insets of Figure 2a (SAED) and Figure 2b (FFT) show that each Ag_2S nanoparticle is single-crystalline in structure. The lattice spacings of 0.209, 0.225, and 0.201 nm in Figure 2b match well with the interplanar distances of $(\bar{1}22)$, $(11\bar{3})$, and $(2\bar{1}\bar{1})$ planes of the monoclinic Ag_2S, respectively, which also can be illustrated by the corresponding FFT pattern along the [453] zone axis (inset in Figure 2b). EDS spectra (Figure 2c) show Ag and S with an Ag:S atomic ratio of nearly 2, in good agreement with the stoichiometric Ag_2S. Figure 2d shows the histogram of Ag_2S particle size distribution of the same sample. The diameters of Ag_2S nanoparticles were in the range of 36−54 nm; the average diameter of Ag nanoparticles was 43.8 ± 1.7 nm (1.7 nm is the standard deviation). The particle size distribution is approximately fit the Gaussian curve. Microwave irradiation results in a homogeneous fast heating. Thus, Ag^+ ions are rapidly reduced to Ag^0 and react with melted S in the whole system, leading to a rapid nucleation at the same time, which is a beneficial factor to the formation of nanosized and well-dispersed colloidal Ag_2S nanoparticles. Our previous results showed that the synthesis of PAM cannot be conducted by the conventional oil bath method at 125 °C in a short period of time, unless a much longer reaction time (about 2.5 h) was used.[20]

PAM−Ag_2S nanocomposite with larger Ag_2S average particle size and broader particle size distribution was obtained by microwave heating at 125 °C for a longer reaction time (60 min) or at a higher temperature (190 °C) for 15 min (Figures 3 and 4). For example, the average particle size of Ag_2S was 56.8 ± 7.9 nm for the PAM−Ag_2S nanocomposite prepared by microwave heating at 125 °C for 60 min (Figure 3b). The broader particle size distribution and larger Ag_2S average particle size may be ascribed to continuous growth of Ag_2S crystals through Ostwald ripening in which bigger crystals continuously grow at the expense of smaller ones. Temperature has a significant influence on the particle size of Ag_2S. The average particle size of Ag_2S increased from 43.8 ± 1.7 to 81.4 ± 14.8 nm when the temperature increased from 125 (Figure 2d) to 190 °C (Figure 4b). This difference may be attributed to aggregation and fast growth of Ag_2S crystals induced by higher reaction temperature. Figure 5 shows the TEM micrograph of the PAM−Ag_2S nanocomposite prepared by microwave heating an EG (50 mL) solution containing 10 mmol of $AgNO_3$, 10 mmol of S, and 0.15 mol of AM at 125 °C for 15 min. The average particle size of Ag_2S was increased with increasing concentration of $AgNO_3$ due to the higher growth rate of Ag_2S crystals at higher concentration of reactants. Because of the higher concentration of reactants, the nucleation of Ag_2S continued during the Ag_2S crystal growth, resulting in a wider Ag_2S particle size distribution.

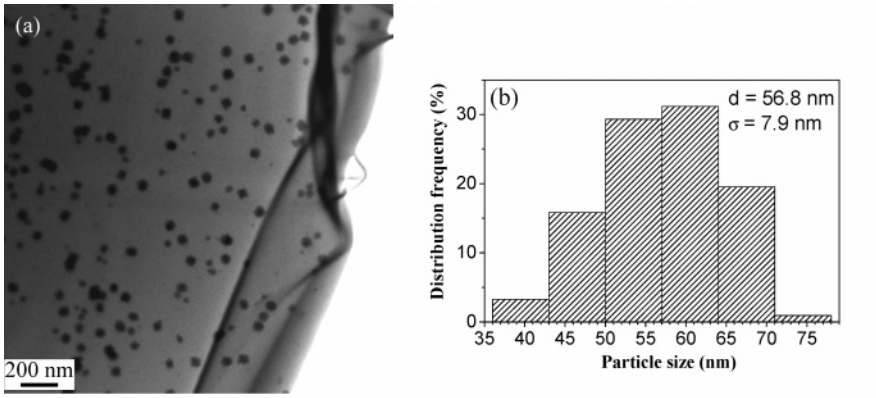

Figure 3. TEM micrograph (a) and the histogram of Ag_2S particle size distribution (b) of PAM−Ag_2S nanocomposite prepared by microwave heating an EG (50 mL) solution of 2 mmol of $AgNO_3$, 2 mmol of S, and 0.15 mol of AM at 125 °C for 60 min.

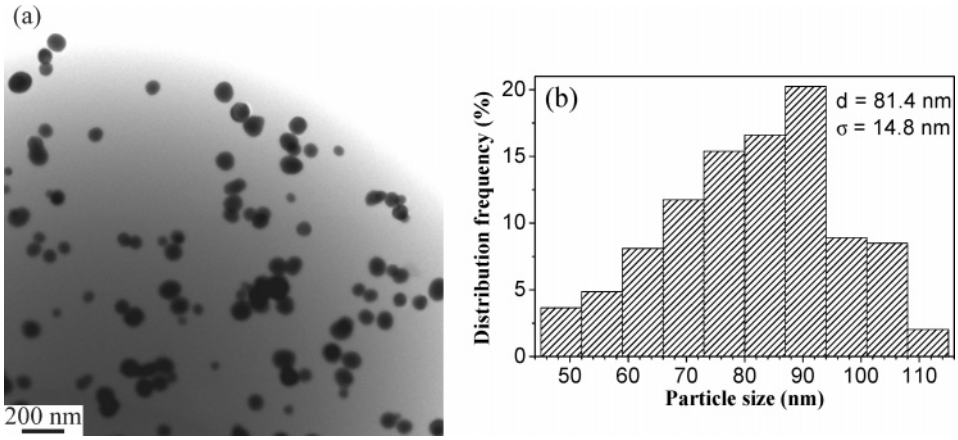

Figure 4. TEM micrograph (a) and the histogram of Ag_2S particle size distribution (b) of PAM−Ag_2S nanocomposite prepared by microwave heating an EG (50 mL) solution of 2 mmol of $AgNO_3$, 2 mmol of S, and 0.15 mol of AM at 190 °C for 15 min.

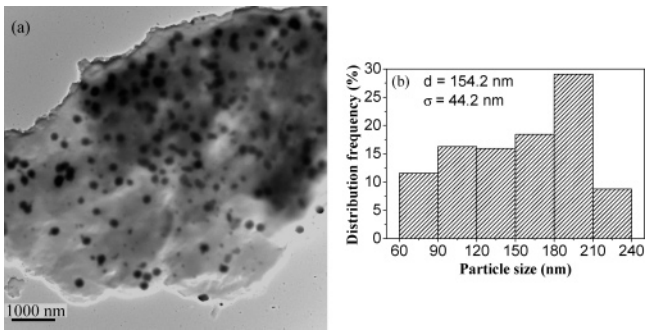

Figure 5. TEM micrograph (a) and the histogram of Ag_2S particle size distribution (b) of PAM−Ag_2S nanocomposite prepared by microwave heating an EG (50 mL) solution of 10 mmol of $AgNO_3$, 10 mmol of S, and 0.15 mol of AM at 125 °C for 15 min.

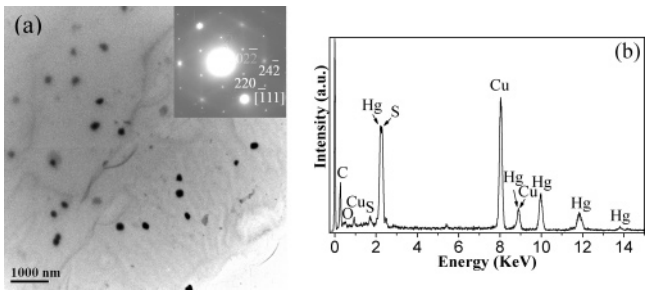

Figure 6. (a) TEM micrograph of the PAM−HgS nanocomposite prepared by microwave heating an EG (50 mL) solution containing 1 mmol of $Hg(NO_3)_2 \cdot H_2O$, 2 mmol of S, and 0.15 mol of AM at 190 °C for 15 min. The upper inset shows the selected area electron diffraction (SAED) pattern of an individual HgS particle. (b) EDS spectrum of the PAM−HgS nanocomposite.

TEM images of PAM−HgS and PAM−Cu_2S nanocomposites prepared by the microwave-assisted method are shown in Figures 6 and 7, respectively. One can see that HgS particles with sizes between 150 and 250 nm are well dispersed in PAM. SAED (inset of Figure 6a) shows that HgS particles are single-crystalline in structure. EDS (Figure 6b) shows that the sample consists of Hg and S and the ratio of Hg:S is very close to 1, indicating that the chemical composition is HgS. Figure 7a shows Cu_2S nanoparticles, and aggregates with sizes between 5 and 40 nm are dispersed in PAM. The morphologies of Cu_2S particles are irregular, including sphere, ellipse, rod, and rectangle. The EDS spectrum (Figure 7b) shows the ratio of Cu:S is 2:1, indicating the formation of Cu_2S, not CuS and Cu.

To verify the formation of PAM in the nanocomposite product, the FTIR spectra of pure PAM and PAM−Ag_2S nanocomposite were studied, as shown in Figure 8. The strong double peaks at ∼1085 and ∼1040 cm^{-1} should belong to the stretching vibration of C−O in the $-CH_2-OH$ group of the solvent EG (Figure 8a). The strong peak at ∼890 cm^{-1} assigned to $=CH_2$ appears only in the spectrum of the monomer AM (Figure 8a) and vanishes in the spectrum of the PAM and PAM−Ag_2S nanocomposite (Figure 8b and c), which confirms that AM monomer has successfully polymerized under microwave irradiation. The spectra of the pure PAM and PAM−Ag_2S nanocomposite are similar and consistent with the standard infrared spectrum of PAM.[21] The N−H stretching vibrations were observed at ∼3413 and ∼3201 cm^{-1}. The strong absorp-

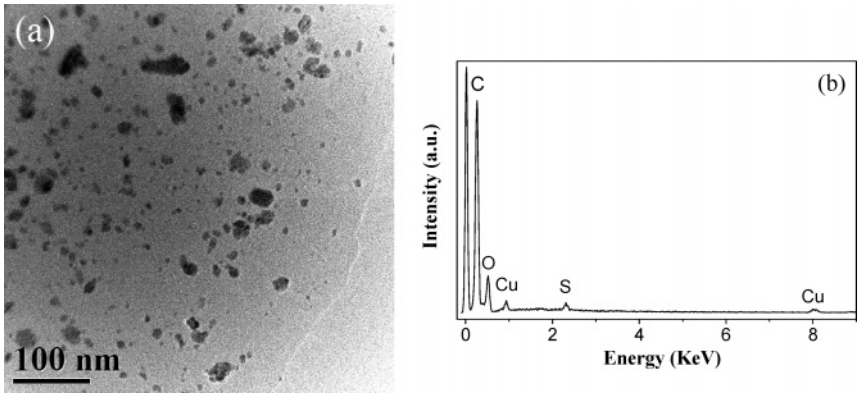

Figure 7. (a) TEM micrograph of the PAM−Cu_2S nanocomposite prepared by microwave heating an EG (50 mL) solution of 2 mmol of $Cu(NO_3)_2 \cdot 3H_2O$, 2 mmol of S, and 0.15 mol of AM at 190 °C for 15 min; and (b) EDS spectrum of the PAM−Cu_2S nanocomposite.

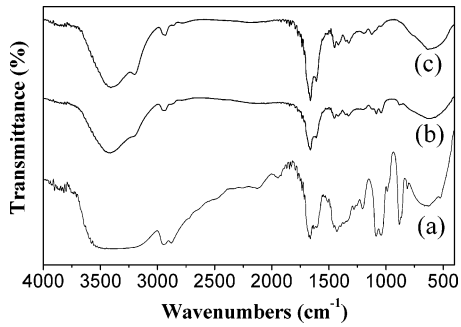

Figure 8. FTIR spectra of: (a) the EG (50 mL) solution containing 2 mmol of $AgNO_3$, 2 mmol of S, and 0.15 mol of AM; (b) PAM prepared by microwave heating an EG (50 mL) solution containing 0.15 mol of AM at 125 °C for 15 min; and (c) PAM−Ag_2S nanocomposite prepared by microwave heating the same solution as in (a) at 125 °C for 15 min.

tion at ∼1662 cm^{-1} can be attributed to the C═O stretching in the $-CONH_2$ group, and the shoulder around ∼1608 cm^{-1} to the NH_2 bending. The characteristic peak at ∼2931 cm^{-1} is assigned to $-CH_2-$ stretching. The peaks at ∼1450 and ∼1415 cm^{-1} are assigned to δ_{-CH_2-}.

The generation of metal sulfide nanoparticles could also be identified from both the color change and the UV−vis spectra of the as-prepared nanocomposites. Pure colorless transparent PAM solution exhibited no absorption in the visible region (Figure 9a). Each spectrum of PAM−Ag_2S nanocomposites shows a gradual increase in absorption toward shorter wavelength. As compared to the band gap of bulk Ag_2S (1 eV, 1240 nm),[22] the apparent blue shift of the observed absorption in Figure 9b indicates that the Ag_2S nanoparticles may be near or within the quantum confinement regime. From Figure 9b to e, the blue shift of the absorption gradually lessens, due to the increasing average particle size of Ag_2S in the nanocomposites from 43.8 ± 1.7 to 154.2 ± 44.2 nm. The absorption plots become broader in visible region as Ag_2S size distributions become broader from Figure 9b to e. This phenomenon is likely due to the overlap of absorption bands at different energies arising from Ag_2S nanocrystals with different sizes. These results are consistent with the TEM observation. The absorption spectrum of copper sulfide is indeed very handy in the determination of its phase.[23] From Figure 9f, it is inferred that the phase of copper sulfide obtained in the nanocomposite is Cu_2S rather than CuS, as it does not show the characteristic absorption of CuS in the near IR region (ca. 920 nm), which is hardly affected by the size of the particles.[23−26] As compared to the band gaps of bulk Cu_2S (∼1022 nm)[23,25] and β-HgS (2.0 eV, 620 nm),[5] there are distinct blue shifts of the observed

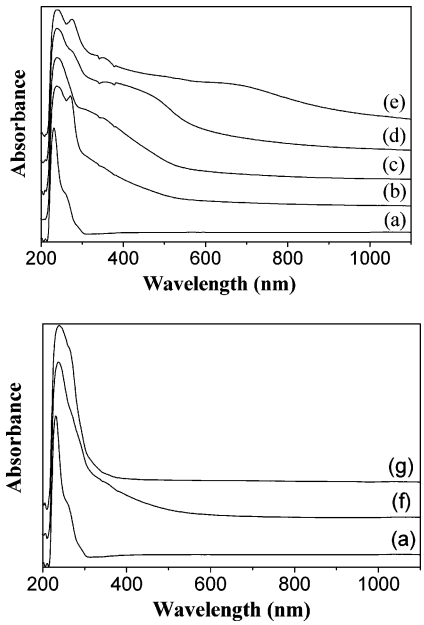

Figure 9. UV−vis absorption spectra of a colloidal solution prepared by microwave heating an EG (50 mL) solution containing (a) 0.15 mol of AM at 125 °C for 15 min; (b) 2 mmol of $AgNO_3$, 2 mmol of S, and 0.15 mol of AM at 125 °C for 15 min; (c) 2 mmol of $AgNO_3$, 2 mmol of S, and 0.15 mol of AM at 125 °C for 60 min; (d) 2 mmol of $AgNO_3$, 2 mmol of S, and 0.15 mol of AM at 190 °C for 15 min; (e) 10 mmol of $AgNO_3$, 10 mmol of S, and 0.15 mol of AM at 125 °C for 15 min; (f) 2 mmol of $Cu(NO_3)_2 \cdot 3H_2O$, 2 mmol of S, and 0.15 mol of AM at 190 °C for 15 min; and (g) 1 mmol of $Hg(NO_3)_2 \cdot H_2O$, 2 mmol of S, and 0.15 mol of AM at 190 °C for 15 min.

absorption in Figure 9f and g due to the size quantization effect of the Cu_2S and β-HgS nanoparticles in the nanocomposites. In contrast to metal sulfides prepared from the solution by microwave heating in the absence of PAM, all of the nanocomposite colloidal solutions show almost no change in UV−vis absorption spectra after storage for 3 months, suggesting the nonaggregation and high stability of metal sulfide nanoparticles in these nanocomposite colloidal solutions under the PAM protection. In addition, the nanocomposite powders collected from the colloidal solutions could be easily redispersed in EG to form the stable colloids by simple agitation for a few minutes. The UV−vis absorption spectra of redispersed colloidal solutions were very similar to those of the newly prepared colloids, implying that metal sulfide nanoparticles did not aggregate after a cycle of drying to powder and redispersion in EG. This advantage is important for convenient storage, transportation, and application of the nanocomposite materials.

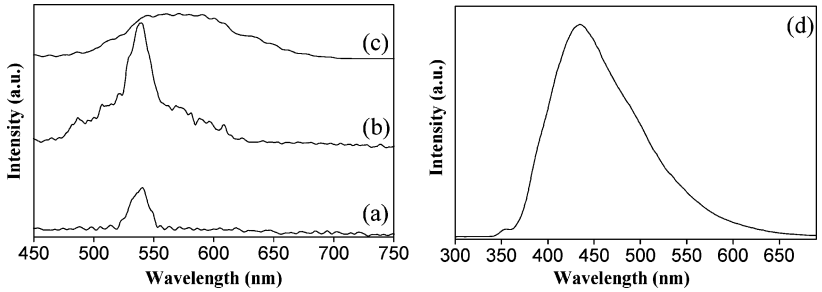

Figure 10. PL spectra of colloidal solutions prepared by microwave heating an EG (50 mL) solution containing: (a) 2 mmol of $AgNO_3$, 2 mmol of S, and 0.15 mol of AM at 125 °C for 15 min; (b) 2 mmol of $AgNO_3$, 2 mmol of S, and 0.15 mol of AM at 125 °C for 60 min; (c) 2 mmol of $AgNO_3$, 2 mmol of S, and 0.15 mol of AM at 190 °C for 15 min; and (d) 1 mmol of $Hg(NO_3)_2 \cdot H_2O$, 2 mmol of S, and 0.15 mol of AM at 190 °C for 15 min.

The PL spectra of the PAM−Ag_2S colloidal solutions were obtained with the excitation wavelength of 400 nm. Figure 10a shows the PL spectrum of PAM−Ag_2S colloidal solution prepared at 125 °C for 15 min; one can see an emission peak centered at ∼540 nm. As compared to Figure 10a, the emission peak in Figure 10b centered at a similar wavelength, which may be interpreted that the peak position of the PL spectra is mainly contributed by the smaller Ag_2S particles with similar sizes in the two samples.[27] The peak width is obviously broadened in Figure 10b due to a wider size distribution of Ag_2S particles in this sample. The emission peak is red-shifted and further broadened in Figure 10c because of increased particle size and broadened size distribution of Ag_2S particles. The PL of the PAM−Ag_2S colloidal solution prepared using higher concentrations of reactants (10 mmol of $AgNO_3$ and 10 mmol of S) was not observed in the visible region due to large particle size of Ag_2S. The large size of Ag_2S particles makes the emission close to the bulk energy level corresponding to near IR. On the other hand, the luminescence yield decreases with increasing size of the particles.[27] These results are consistent with those obtained from TEM and UV−vis absorption spectra. The PL spectrum of the PAM−HgS colloidal solution was measured at the excitation wavelength of 350 nm (Figure 10d); it shows a strong emission peak at ∼435 nm, which is similar to the PL spectrum of HgS nanoparticles in other polymer matrix.[5] The PL emission of the PAM−Cu_2S nanocomposite was not detectable in this study.

TG curves of pure PAM and PAM−metal sulfide nanocomposites are given in Figure 11. The overall weight loss in all samples can be roughly divided into three regions depending on the temperature. The first slow weight loss below 250 °C can be assigned to the loss of adsorbed water in PAM.[28] The second weight loss between 250 and 330 °C may correspond to the evolution of NH_3.[29] The third weight loss appears sharply above 350 °C due to the pyrolysis of the imides formed during the second stage.[30] After the TG measurement, a black residue was left. It should be mentioned that the content of metal sulfide in the nanocomposite was very low, and hence the evolvement of the TG curve of the nanocomposite arises mainly from PAM degradation. From Figure 11a to c, the effect of the Ag_2S content on the thermal stability of PAM is presented. The TG curves of the PAM−Ag_2S nanocomposites (Figure 11b and c) are higher than and right of that of pure PAM (Figure 11a). In other words, the temperature for pyrolysis of the same amount of PAM is higher for PAM−Ag_2S than for pure PAM. It should be noticed that the residual mass at 600 °C is 48% for PAM−Ag_2S (1 mmol), while it is 16% for pure PAM. This siginificant difference in residual mass of two samples cannot be simply ascribed to the residual Ag_2S, because the theoretical content of Ag_2S in PAM−Ag_2S (1 mmol) is 2.27 wt %. This implies

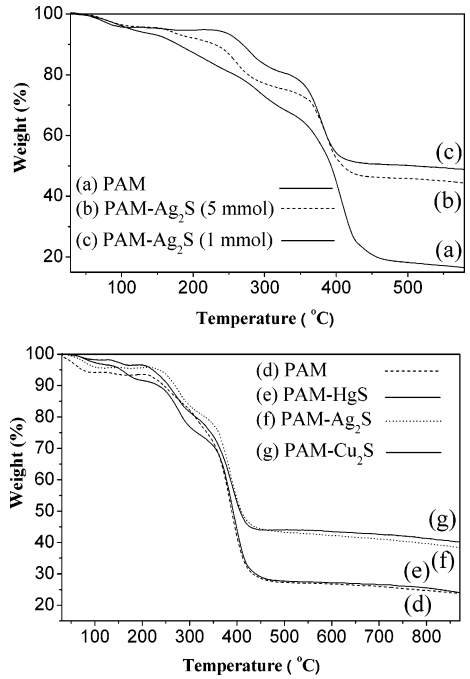

Figure 11. (a)−(c) TG curves of some samples prepared by microwave heating at 125 °C for 15 min: (a) pure PAM; (b) and (c) PAM−Ag_2S nanocomposites with different Ag_2S content, (b) 5 mmol of Ag_2S; (c) 1 mmol of Ag_2S. (d)−(g) TG curves of some samples prepared by microwave heating at 190 °C for 15 min: (d) pure PAM; (e) PAM−HgS; (f) PAM−Ag_2S; and (g) PAM−Cu_2S.

that the small amount of Ag_2S nanoparticles in the nanocomposite hinders the decomposition of PAM. These results indicate that the thermal stability of PAM can be enhanced by the presence of a small amount of Ag_2S nanoparticles as nanofiller. Similar results were also reported for polystyrene−CdS[2] and polystyrene−HgS[31] nanocomposites. The degradation of the polymer usually starts with free radical formations at weak bonds and/or chain ends, followed by their transfer to adjacent chains via interchain reactions. Hence, the observed effect can be explained by the reduced mobility of the PAM chains attached to the surface of the Ag_2S nanoparticles. It is interesting to point out that the effect of Ag_2S nanoparticles on the thermal stability of PAM was slightly reduced as the Ag_2S content was increased (Figure 11b). It may be ascribed to the weak interaction between the PAM and the larger Ag_2S particles with lower surface area in PAM−Ag_2S (5 mmol) than that in PAM−Ag_2S (1 mmol). To access the effect of different nanofillers, TG analysis of pure PAM and PAM−metal sulfide (Ag_2S, HgS, and Cu_2S) nanocomposites prepared at 190 °C was carried out, as shown in Figure 11d−g. It can be seen that the thermal stability of PAM was similarly enhanced by both Ag_2S and Cu_2S nanoparticles

as nanofillers (Figure 11f and g), but hardly affected by HgS (Figure 11e). This may be partly related to the lower surface area of larger HgS particles in PAM−HgS.

In the preparation method reported here, the sulfur powder is melted in the reaction solution at above 115 °C, which is important for the subsequent homogeneous reaction to form relatively uniformly sized metal sulfide nanoparticles. Polymerization of AM is rapidly realized in EG at above 120 °C by microwave heating. The C═C bond in the AM monomer readily absorbs the microwave energy to form the excited state of the monomer M*, and then decomposes to radicals, leading to the polymerization of AM. This process can be facilitated in the EG solvent, which has a high dielectric loss constant (41.0) and absorbs microwave efficiently.[17] EG also serves as a reductant for the formation of metal atoms under microwave irradiation.[17] The metallic atoms quickly react with the soluble S to form metal sulfide nanoparticles. The metal sulfide nanoparticles can be produced as the following reactions:

$$CH_2OH-CH_2OH \rightarrow CH_3CHO + H_2O \quad (1)$$

$$2nCH_3CHO + 2M^{n+} \rightarrow 2M + 2nH^+ + nCH_3COCOCH_3 \quad (2)$$

$$nM + S \rightarrow M_nS \quad (3)$$

It should be noted that sulfur usually cannot oxidize Cu to Cu^{2+} in EG, but to Cu^+, which has been demonstrated in this study. The high viscosity of the system due to the polymerization of AM prevents the movement, growth, and aggregation of nanosized metal sulfides. On the other hand, PAM also acts as a stabilizer for nanoparticles. PAM that contains an O═C−N group may be attached to the surface of metal sulfide nanocrystals through coordination linkage, which lowers the surface free energy of metal sulfide nanoparticles, leading to restriction of the growth and aggregation of nanoparticles. This was also testified by the high stability of the PAM−metal sulfide colloidal solutions and the improved thermal stability of the PAM−metal sulfide nanocomposites.

Conclusion

In summary, microwave heating provides a rapid, convenient, and efficient method for one-step synthesis of PAM−metal sulfide nanocomposites. This novel preparation method is based on the simultaneous formation of the colloidal metal sulfide nanoparticles and the polymerization of the AM monomer in EG solution. Nanosized metal sulfide particles with a narrow size distribution can be homogeneously dispersed in the PAM matrix. EG acts as a solvent, a microwave absorber, and a reductant at the same time. No additional initiator, surfactant, and stabilizer are necessary in the synthesis, which is beneficial to the low-cost production of high-purity nanocomposites. As compared to pure PAM, the thermal stability of PAM−Ag_2S and PAM−Cu_2S nanocomposites is improved. This method reported here may be extended to synthesize other polymer−metal sulfide nanocomposites.

Acknowledgment. Financial support from the National Natural Science Foundation of China (50472014) and the Chinese Academy of Sciences under the Program for Recruiting Outstanding Overseas Chinese (Hundred Talents Program) is gratefully acknowledged. This work was also supported by the K. C. Wong Education Foundation of Hong Kong (20051013194651), the Program of Shanghai Postdoctoral Scientific Research Foundation (05R214148), and the Opening Project of State Key Laboratory of High Performance Ceramics and Superfine Microstructure (SKL200506SIC), Shanghai Institute of Ceramics, Chinese Academy of Sciences.

References and Notes

(1) Caseri, W. *Macromol. Rapid Commun.* **2000**, *21*, 705.

(2) Šajinović, D.; Šaponjić, Z. V.; Cvjetićanin, N.; Marinović-Cincović, M.; Nedeljković, J. M. *Chem. Phys. Lett.* **2000**, *329*, 168.

(3) Liu, S. H.; Qian, X. F.; Yin, J.; Hong, L.; Wang, X. L. *J. Solid State Chem.* **2002**, *168*, 259.

(4) Mu, T.; Du, J.; Li, Z.; Liu, Z.; Han, B.; Wang, J.; Sun, D.; Wang, B. *Colloid Polym. Sci.* **2004**, *282*, 1179.

(5) Sreekumari Nair, P.; Radhakrishnan, T.; Revaprasadu, N. *Macromol. Symp.* **2003**, *193*, 227.

(6) Sreekumari Nair, P.; Radhakrishnan, T.; Revaprasadu, N.; Kolawole, G. A.; Luyt, A. S.; Djoković, V. *Appl. Phys. A* **2005**, *81*, 835.

(7) Xie, Y.; Qiao, Z. P.; Chen, M.; Zhu, Y. J.; Qian, Y. T. *Nanostruct. Mater.* **1999**, *11*, 1165.

(8) Qiao, Z. P.; Xie, Y.; Zhu, Y. J.; Qian, Y. T. *Mater. Sci. Eng., B* **2000**, *77*, 144.

(9) Qiao, Z. P.; Xie, Y.; Zhu, Y. J.; Qian, Y. T. *J. Mater. Chem.* **1999**, *9*, 1001.

(10) Qiao, Z. P.; Xie, Y.; Li, G.; Zhu, Y. J.; Qian, Y. T. *J. Mater. Sci.* **2000**, *35*, 285.

(11) Chen, M.; Xie, Y.; Qiao, Z. P.; Zhu, Y. J.; Qian, Y. T. *J. Mater. Chem.* **2000**, *10*, 329.

(12) Qiao, Z. P.; Xie, Y.; Chen, M.; Xu, J. G.; Zhu, Y. J.; Qian, Y. T. *Chem. Phys. Lett.* **2000**, *321*, 504.

(13) Qiao, Z. P.; Xie, Y.; Xu, J. G.; Zhu, Y. J.; Qian, Y. T. *Mater. Res. Bull.* **2000**, *35*, 1355.

(14) Zhou, Y.; Hao, L. Y.; Hu, Y.; Zhu, Y. R.; Chen, Z. Y. *Chem. Lett.* **2000**, 1308.

(15) He, R.; Qian, X. F.; Yin, J.; Bian, L. J.; Xi, H. A.; Zhu, Z. K. *Mater. Lett.* **2003**, *57*, 1351.

(16) Mastai, Y.; Gedanken, A. Sonochemistry and Other Novel Methods Developed for the Synthesis of Nanoparticles. In *The Chemistry of Nanomaterials: Synthesis, Properties and Application*; Rao, C. N. R., Müller, A., Cheetham, A. K., Eds.; Wiley−VCH Verlag GmbH & Co. KgaA: Weinheim, 2004; Vol. 1, p 152.

(17) Tsuji, M.; Hashimoto, M.; Nishizawa, Y.; Kubokawa, M.; Tsuji, T. *Chem.-Eur. J.* **2005**, *11*, 440.

(18) Zhu, Y. J.; Wang, W. W.; Qi, R. J.; Hu, X. L. *Angew. Chem., Int. Ed.* **2004**, *43*, 1410.

(19) Zhu, Y. J.; Qian, Y. T.; Li, X. J.; Zhang, M. W. *Chem. Commun.* **1997**, 1081.

(20) Zhu, J. F.; Zhu, Y. J. *J. Phys. Chem. B* **2006**, *110*, 8593.

(21) Sprouse, J., Hansen, D., Eds. *Sprouse Collection of Infrared Spectra Book I: Polymers 357*; Sprouse Scientific Systems: Paoli, PA, 1987; Standard Infrared Grating Spectra, Vols. 9−10 (8001−10000), p 8284.

(22) Brelle, M. C.; Zhang, J. Z.; Nguyen, L.; Mehra, R. K. *J. Phys. Chem. A* **1999**, *103*, 10194.

(23) Haram, S. K.; Mahadeshwar, A. R.; Dixit, S. G. *J. Phys. Chem.* **1996**, *100*, 5868.

(24) Silvester, E. J.; Grieser, F.; Sexton, B. A.; Healy, T. W. *Langmuir* **1991**, *7*, 2917.

(25) Zhang, P.; Gao, L. *J. Mater. Chem.* **2003**, *13*, 2007.

(26) Dixit, S. G.; Mahadeshwar, A. R.; Haram, S. K. *Colloids Surf., A* **1998**, *133*, 69.

(27) Pileni, M. P.; Motte, L.; Billoudet, F.; Mahrt, J.; Willig, F. *Mater. Lett.* **1997**, *31*, 255.

(28) Rangaraj, A.; Vangani, V.; Rakshit, A. K. *J. Appl. Polym. Sci.* **1997**, *66*, 45.

(29) Yang, M. H. *Polym. Test.* **1998**, *17*, 191.

(30) Yang, M. H. *J. Appl. Polym. Sci.* **2002**, *86*, 1540.

(31) Sreekumari Nair, P.; Radhakrishnan, T.; Revaprasadu, N.; van Sittert, C. G. C. E.; Djoković, V.; Luyt, A. S. *Mater. Lett.* **2004**, *58*, 361.